Solar Cells Based on Quantum Dots: Multiple Exciton Generation and Intermediate Bands

Antonio Luque, Antonio Martí, and Arthur J. Nozik

Abstract

Semiconductor quantum dots may be used in so-called third-generation solar cells that have the potential to greatly increase the photon conversion efficiency via two effects: (1) the production of multiple excitons from a single photon of sufficient energy and (2) the formation of intermediate bands in the bandgap that use sub-bandgap photons to form separable electron–hole pairs. This is possible because quantization of energy levels in quantum dots produces the following effects: enhanced Auger processes and Coulomb coupling between charge carriers; elimination of the requirement to conserve crystal momentum; slowed hot electron–hole pair (exciton) cooling; multiple exciton generation; and formation of minibands (delocalized electronic states) in quantum dot arrays. For exciton multiplication, very high quantum yields of 300–700% for exciton formation in PbSe, PbS, PbTe, and CdSe quantum dots have been reported at photon energies about 4–8 times the HOMO–LUMO transition energy (quantum dot bandgap), respectively, indicating the formation of 3–7 excitons/photon, depending upon the photon energy. For intermediate-band solar cells, quantum dots are used to create the intermediate bands from the confined electron states in the conduction band. By means of the intermediate band, it is possible to absorb below-bandgap energy photons. This is predicted to produce solar cells with enhanced photocurrent without voltage degradation.

Introduction

This article summarizes and reviews the application of quantization effects in semiconductor nanocrystals to produce third-generation quantum dot (QD) solar cells that can deliver solar electricity at very low cost. The establishment of an extremely low-cost goal of \$0.02–\$0.04/kWh for solar power requires a cell conversion efficiency of about 50% but with a total cost of \$125/m^2. Such combinations of cost and efficiency require truly disruptive technologies that do not exist at the present time. However, the attainment of these goals does not conflict with nor violate any fundamental scientific principles and is theoretically feasible.

Here, we discuss two approaches based on semiconductor quantum dots and quantum dot arrays that could lead to ultrahigh efficiencies through enhanced photocurrent. One approach is based on using high-energy photons in the solar spectrum to create multiple electron–hole pairs from single photons; the second is based on the formation of an intermediate band (IB) within the semiconductor bandgap that enables the absorption of sub-bandgap photons to excite electrons from the valence band to the IB followed by the absorption of a second sub-bandgap photon to excite the electrons in the IB to the conduction band.

Approach

As is well known, the maximum thermodynamic efficiency for the conversion of unconcentrated solar irradiance into electrical free energy in the radiative limit, assuming detailed balance, a single threshold absorber, and thermal equilibrium between electrons and phonons, was calculated by Shockley and Queisser in 1961[1] to be about 31%. For full solar concentration (46,300 suns), the maximum single-bandgap efficiency increases to about 41%.

In the Shockley–Queisser analysis, two major factors limit the conversion efficiency to 31%: (1) the excess kinetic energy of hot photogenerated carriers created by the absorption of supra-bandgap photons is lost as heat through phonon emission, and (2) photons less than the bandgap are not absorbed. The first approach to third-generation solar cells discussed here addresses the first factor in the Shockley–Queisser analysis (thermalization loss of hot electrons), whereas the second approach addresses the second factor (loss of sub-bandgap photons).

Multiple-Exciton-Generation Solar Cells

There are two fundamental ways to prevent the thermalization loss produced from the absorption of high-energy photons above the bandgap in a single-bandgap system. One way produces an enhanced photovoltage; the other way produces an enhanced photocurrent. The former requires that the hot carriers be extracted from the photoconverter before they cool,[2–4] whereas the latter requires the hot carriers to produce two or more electron–hole pairs;[5,6] in QDs this is known as multiple exciton generation (MEG).[7] The former process results in a thermodynamic limit at 1 sun of about 66%, whereas the latter produces a thermodynamic limit of about 45%.[8] At full solar concentration (46,300 suns), both approaches converge at 86% conversion efficiency. The latter process is well known in bulk semiconductors and is termed impact ionization; it is the inverse of the Auger process whereby one of two electron–hole pairs recombines to produce a single highly energetic electron–hole pair.

Intermediate-Band Solar Cells

To capture and use photons less than the bandgap energy, IB solar cells can be used that are based on the so-called intermediate-band materials.[9] These materials are characterized by the existence of an intermediate band located between the conventional semiconductor conduction band (CB) and valence band (VB) (Figure 1).

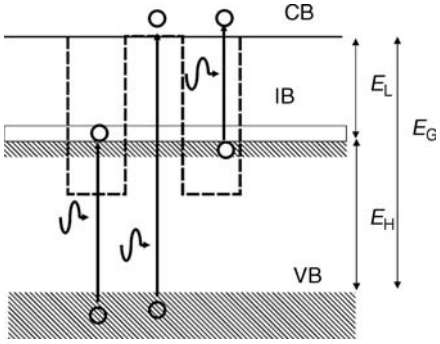

Figure 1. Structure of an intermediate-band (IB) material, showing the possible optical transitions. The dashed lines in the bandgap (E_G) represent the formation of the IB from an array of quantum dots. CB is conduction band, VB is valence band.

Because of the IB, below-bandgap-energy photons can contribute to the cell photocurrent by pumping electrons from the VB to the IB and from the IB to the CB. But most importantly, because the IB is isolated from the CB and the VB by a zero density of states, "carrier relaxation" between bands becomes difficult and the carrier statistics in each band is described by its own quasi-Fermi level. It can be shown that, under this assumption, the voltage supplied by the cell, given by the electron–hole quasi-Fermi level split, is still limited by the high bandgap E_G and not by any of the lower bandgaps (E_L or E_H). The study of the limiting photovoltaic conversion efficiency of the IB approach reveals a limiting efficiency[9,10] of ~47% at 1 sun (~63% at full solar concentration) for this concept, as compared with ~43% for a two-gap tandem solar cell at 1 sun (~55% for full solar concentration).

Electron–Hole Pair Multiplication in Quantum Dots

The formation of multiple electron–hole pairs per absorbed photon by impact ionization in bulk semiconductors has not contributed meaningfully to improved quantum yields in working solar cells, primarily because the impact ionization efficiency does not reach significant values until photon energies reach the ultraviolet region of the spectrum. In bulk semiconductors, the threshold photon energy for impact ionization exceeds that required for energy conservation alone, because in addition to conserving energy, crystal momentum must be conserved. Furthermore, the rate of impact ionization must compete with the rate of energy relaxation by electron–phonon scattering. It has been shown that the rate of impact ionization becomes competitive with phonon scattering rates only when the kinetic energy of the electron is many times the bandgap energy E_g.[11–13] Thus, in Si the impact ionization efficiency was found to be only 5% (i.e., total quantum yield = 105%) at a photon energy $h\nu \approx 4$ eV ($3.6 \times E_g$), and 25% at $h\nu \approx 4.8$ eV ($4.4 = E_g$).[14,15] This large blueshift of the threshold photon energy for impact ionization in semiconductors prevents materials such as bulk Si and GaAs from yielding improved solar conversion efficiencies.[6,15]

However, in quantum dots, the rate of Auger processes, including the inverse Auger process of exciton multiplication, is greatly enhanced because of carrier confinement and the concomitantly increased electron–hole Coulomb interaction (see Figure 2). Furthermore, crystal momentum need not be conserved because momentum is not a good quantum number for three-dimensionally–confined carriers. Indeed, very efficient multiple electron–hole pair generation (MEG) by one photon has been reported recently in PbSe, PbS, PbTe, and CdSe nanocrystals.[7,16–20] A quantum yield of 300% was reported for 3.9-nm-diameter PbSe quantum dots at a photon energy of 4 E_g, indicating the formation of three excitons per photon for every photoexcited QD in the sample, and 700% quantum yield was reported in PbSe at an excitation energy of eight times the bandgap.[19] A new possible mechanism for MEG was also introduced that invokes a coherent superposition of multiple excitonic states, meaning that multiple excitons are essentially created instantly upon absorption of high-energy photons.[7,18] Other models to explain MEG have also been published recently.[21,22]

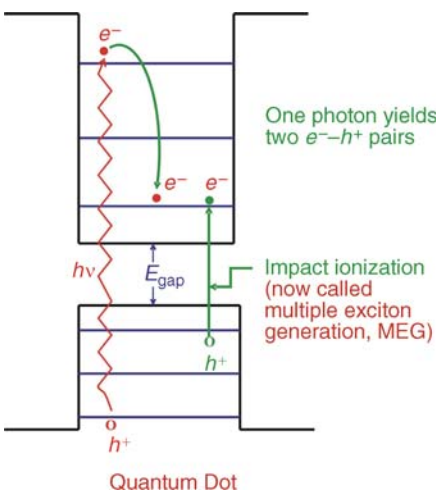

Figure 2. Enhanced electron–hole pair (exciton) multiplication in quantum dots that could lead to enhanced solar photon conversion efficiency in QD solar cells. (From Reference 48.)

Multiexcitons are detected by monitoring the signature of multiexciton decay dynamics using transient absorption spectroscopy of the photoinduced absorption change at the band edge, which is proportional to the number of electron–hole pairs created in the sample.[7,16] The transients are detected by probing either with a band edge (energy gap or HOMO–LUMO transition energy $\equiv E_g$) probe pulse, or with a mid-infrared probe pulse that monitors intraband transitions in the newly created excitons.[7]

In Figure 3, the dependence of the MEG quantum yield on the ratio of the pump photon energy to the bandgap ($E_{h\nu}/E_g$) varies from 1.9 to 5.0 for PbSe quantum dot samples with $E_g = 0.73$ eV (diameter = 5.7 nm), $E_g = 0.82$ eV (diameter = 4.7 nm), and $E_g = 0.91$ eV (diameter = 3.9 nm). The data show, for example, that for the 3.9-nm QD ($E_g = 0.91$ eV), the quantum yield reaches a remarkable value of 300% at $E_{h\nu}/E_g = 4.0$, indicating that the quantum dots produce three excitons per absorbed photon. The data also showed that the quantum yield begins to surpass 100% at $E_{h\nu}/E_g$ values > 2.0 (see Figure 3).

Quantum Dot Solar Cells

The two fundamental pathways for enhancing the conversion efficiency (increased photovoltage[2–4] or increased photocurrent[2,5,6]) can be accessed, in principle, in three different QD solar cell configurations; these configurations are shown in Figure 4 and described here. However, it is emphasized that although 300% quantum yield was measured for exciton formation in the QDs, no group has yet reported enhanced photocurrent with photocurrent quantum yields greater than 100% in any QD-based photon conversion device where the multiple excitons are dissociated and the electron and holes separated and collected in an external circuit. Such experiments are currently in progress. Thermodynamic calculations[8] based on detailed balance show that at 1 sun the upper conversion efficiency limit for MEG with a quantum yield of 200% is 42%; with a quantum yield of 300% the limit is 43%. Thus, most of the efficiency gain above the Shockley–Queisser 31% limit is obtained with just 2 excitons/photon.

Some specific QD cell configurations being investigated are

- **Photoelectrodes composed of QD arrays.** In this configuration, the QDs are formed into an ordered three-dimensional (3D) array with inter-QD spacing sufficiently small such that strong electronic coupling

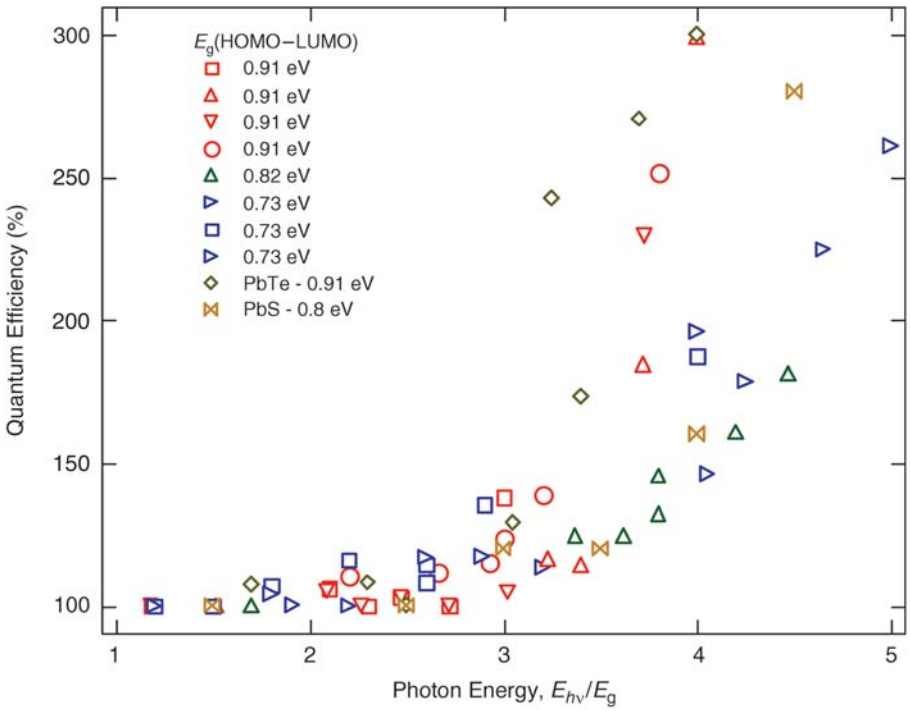

Figure 3. Quantum efficiency for exciton formation from a single photon versus photon energy expressed as the ratio of the photon energy to the quantum dot bandgap (HOMO–LUMO energy) for three PbSe QD sizes (diameters, 3.9, 4.7, and 5.4 nm), one PbS and PbTe size (diameter, 5.5 nm for both), and bandgap energy E_g = 0.91 eV, 0.82 eV, 0.73 eV, 0.85 eV, and 0.91 eV, respectively). Data acquired using a mid-infrared probe or a band-edge probe energy are combined, and the results were independent of the probe energy used. (From References 7 and 17.)

occurs and minibands are formed to enable long-range electron transport (see Figure 4a). The system is a 3D analog to a 1D superlattice and the miniband structures formed therein.[2] The delocalized quantized 3D miniband states could be expected to slow the carrier cooling and permit the transport and collection of hot carriers to produce a higher photopotential in a photovoltaic cell or in a photoelectrochemical cell where the 3D QD array is the photoelectrode. Also, impact ionization might be expected to occur in the QD arrays, enhancing the photocurrent.

■ **QD-sensitized nanocrystalline TiO_2 solar cells.** This configuration is a variation of a recent promising new type of photovoltaic cell that is based on dye-sensitization of nanocrystalline TiO_2 layers.[23–25] In this photovoltaic cell, dye molecules are chemisorbed onto the surface of 10–30-nm TiO_2 particles that have been sintered into a highly porous, nanocrystalline, 10–20-μm TiO_2 film. Upon photoexcitation of the dye molecules, electrons are very efficiently injected from the excited state of the dye into the conduction band of the TiO_2, affecting charge separation and producing a photovoltaic effect.

For the QD-sensitized cell, QDs are substituted for the dye molecules (see Figure 4b); they can be adsorbed from a colloidal QD solution[24] or produced *in situ*.[27–30]

Successful PV effects in such cells have been reported for several semiconductor QDs, including InP, CdSe, CdS, and PbS.[26–30] Possible advantages of QDs as compared with dye molecules are efficient MEG, the tunability of optical properties with size, and better heterojunction formation with solid hole conductors.

■ **QDs dispersed in organic semiconductor polymer matrices.** Recently, photovoltaic effects have been reported in structures consisting of QDs forming junctions with organic semiconductor polymers (see Figure 4c). In one configuration, a disordered array of CdSe QDs is formed in a hole-conducting polymer—poly(2-methoxy,5-(2′-ethyl)-hexyloxy-*p*-phenylenevinylene) (MEH-PPV).[31] Upon photoexcitation of the QDs, the photogenerated holes are injected into the MEH-PPV polymer phase and are collected via an electrical contact to the polymer phase. The electrons remain in the CdSe QDs and are collected through diffusion and percolation in the nanocrystalline phase to an electrical contact to the QD network. Initial results show relatively low conversion efficiencies[31,32] but improvements have been reported with rod-like CdSe nanocrystal shapes[33] embedded in poly(3-hexylthiophene) (the rod-like shape enhances electron transport through the nanocrystalline QD phase).

A variation of these configurations is to disperse the QDs into a blend of electron-conducting and hole-conducting polymers (see Figure 4c). This scheme is the inverse of light-emitting diode structures based on QDs. In the photovoltaic cell, each type of carrier-transporting polymer would have a selective electrical contact to remove the respective charge carriers. A critical factor for success is to prevent electron–hole recombination at the interfaces of the two polymer blends; prevention of electron–hole recombination is also critical for the other QD configurations mentioned above.

Intermediate-Band Solar Cells

There are multiple issues behind the IB cell concept that merit a detailed discussion. For this, the reader should refer to some selected references.[34–36] To emphasize one of them, we shall mention the reason, recently discussed in Reference 37, that the introduction of energy levels within the semiconductor bandgap is not expected to create nonradiative recombination centers that reduce the performance of the cell instead of improving it. The fundamental explanation is that the wave function associated with the electrons in the IB has to be delocalized for the IB to improve efficiency. This is contrary to conventional nonradiative recombination centers, which are tightly bound. Actually, the term "band" in the IB concept is used to emphasize this aspect.

QDs have been proposed[38] as one of the means of manufacturing the IB solar cell. In this respect, the IB would arise from the confined electronic states of the electrons in the potential wells of the conduction band (Figure 1). Delocalization of the electrons in the IB could be achieved by increasing their density until the electron wave functions have significant overlap and become delocalized (Mott transition).[39] This is analogous to the miniband formation illustrated in Figure 4 and discussed above for arrays of QDs.

QDs have the potential to truly isolate the intermediate band from the conduction band by means of a zero density of states. Actually, it is this isolation that is considered to be responsible for the controversial[40–42] "phonon bottleneck" effect through

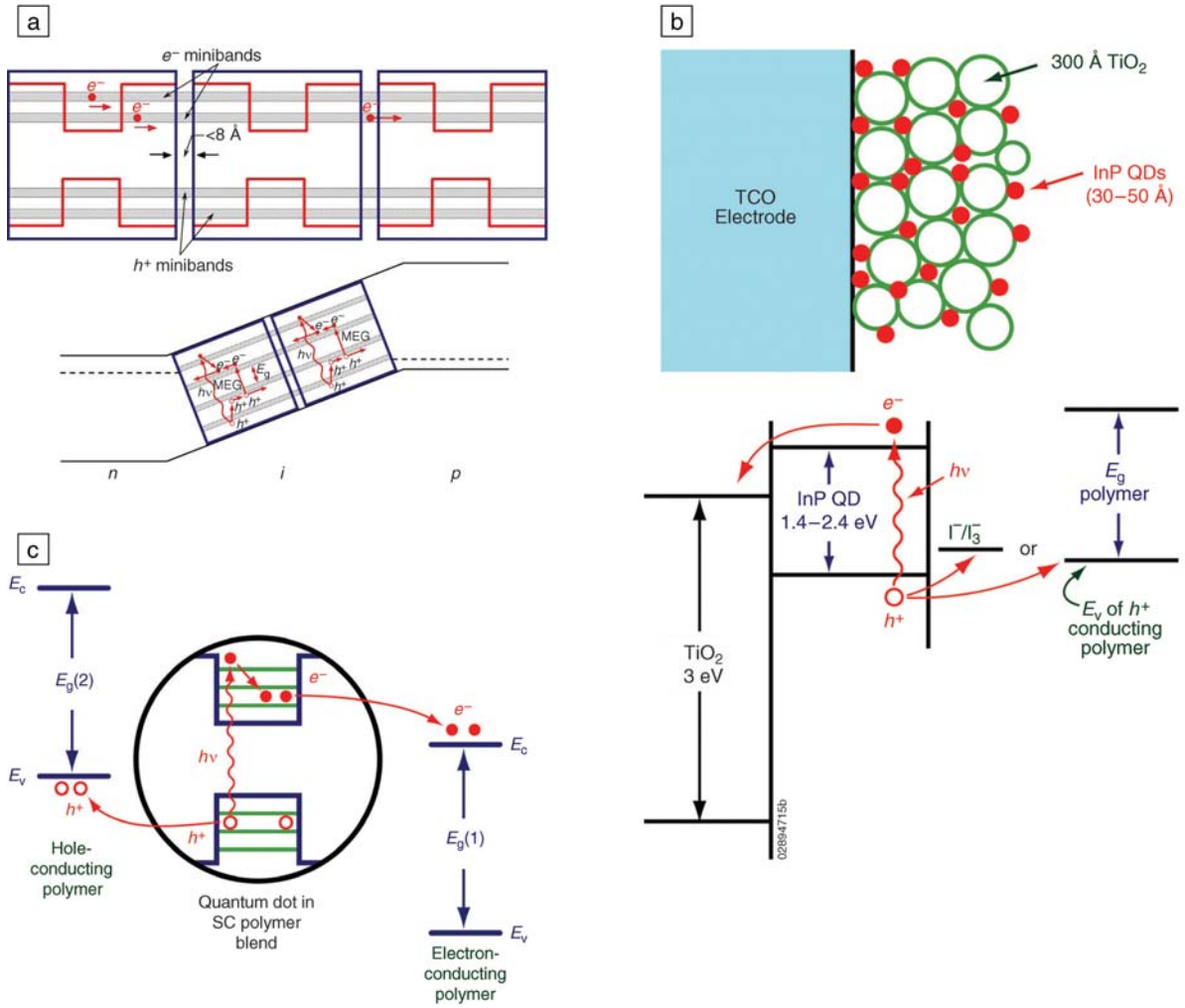

Figure 4. Configurations for quantum dot solar cells. (a) QD array used as a photoelectrode for a photoelectrochemical cell or as the *i*-region of a *p*–*i*–*n* photovoltaic cell; (b) QDs used to sensitize a nanocrystalline film of a wide-bandgap oxide semiconductor (TiO_2) to visible light. This configuration is analogous to the dye-sensitized solar cell where the dye is replaced by QDs. (c) QDs dispersed in a blend of electron- and hole-conducting polymers; SC stands for semiconductor. In (a), (b), and (c), the occurrence of multiple exciton generation (MEG) could produce higher photocurrents and higher conversion efficiency. In (a), enhanced efficiency could be achieved either through MEG or hot carrier transport through the minibands of the QD array, resulting in a higher photopotential. (From Reference 40.)

which a transition from the CB to the IB is believed to be inhibited because of the low probability of simultaneous multiphonon interactions with electrons needed to bridge the energy difference between the CB and the IB.

To facilitate the absorption of photons that cause transitions from the IB to the CB, the IB must be half-filled with electrons so that there are enough electrons to have a reasonable rate of electron promotion from the IB to the CB. This can be accomplished through *n*-type modulation doping of the barrier[43] region between dots at an approximate concentration that equals the dot concentration.

The basic structure of QD–IB solar cell prototype cells consists of 10 layers of InAs/GaAs QDs sandwiched by *p* and *n* GaAs emitters and grown by molecular-beam epitaxy in the Stranski–Krastanov growth mode.[44] Figure 5 shows a typical current–voltage characteristic compared with that of a test GaAs sample. As can be seen, the photogenerated current appears to be approximately the same. However, an examination of the quantum efficiency of the cells (Figure 6) reveals this is not the case. The QD–IB solar cell exhibits an extended response for photon energies lower than the GaAs bandgap. The contribution to the total current of the cell resulting from below-bandgap-energy photons is small (1%). In this case, poor absorption provided by the QDs is unable to overcome the open-circuit voltage loss. The degradation of the open-circuit voltage, contrary to expectations, as discussed earlier, can be partially explained in terms of an effective reduction in the total bandgap of the QD as a result of the existence of the valence-band offset, but it is also likely contributed to by the presence of a higher density of defects, which reduces minority carrier lifetime in the samples containing the dots. Nevertheless, the existence of a split between the quasi-Fermi levels corresponding to the conduction and intermediate bands has been suggested from analysis of the combined data from quantum efficiency and electroluminescence measurements, suggesting that with improved materials, the IB approach can yield improved efficiency.[45–47]

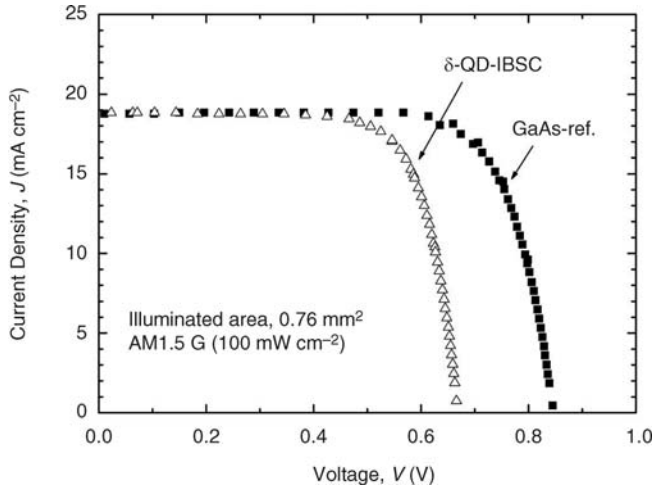

Figure 5. Current–voltage characteristic of a QD intermediate-band solar cell (IBSC) and a reference GaAs solar cell.

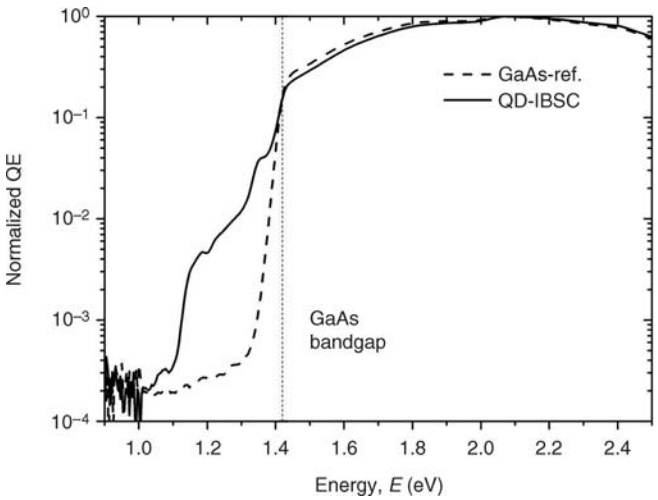

Figure 6. Normalized quantum efficiency (QE) of a QD intermediate-band solar cell (IBSC) compared with that of a reference GaAs solar cell.

Conclusion

The relaxation dynamics of photoexcited excitons in semiconductor quantum dots can be greatly modified compared with the relaxation dynamics of free electron–hole pairs formed in bulk semiconductors. Auger processes are greatly enhanced in quantum dots, and multiple exciton generation (the formation of two or more electron–hole pairs per absorbed photon, called impact ionization in bulk semiconductors) becomes very efficient, and enhanced photocurrents become possible.

Very efficient multiple exciton generation has been observed in PbSe, PbS, PbTe, and CdSe quantum dots; up to 3 excitons/photon have been observed in PbSe QDs at photon energies greater than about four times the QD bandgap (HOMO–LUMO energy separation), and 7 excitons/photon have been reported for excitation at eight times the bandgap. Three types of configurations for QD solar cells are described here that could produce enhanced photocurrent, and the thermodynamic efficiencies for these new types of solar cells have been calculated.

QDs also provide a suitable workbench to study the operating principles of the IB solar cell. Although partial effects have been demonstrated (production of photocurrent for below-bandgap-energy photons and existence of a quasi-Fermi level split), the ultimate demonstration consisting of obtaining an improved photocurrent without voltage degradation remains elusive as a result of, among other factors, the poor absorption provided by the quantum dots.

Acknowledgments

A.J. Nozik was supported by the U.S. Department of Energy, Office of Science, Office of Basic Energy Sciences, Division of Chemical Sciences, Geosciences, and Biosciences. A.J. Nozik acknowledges the vital contributions to the work reviewed here by Randy Ellingson, Matt Beard, Justin Johnson, Olga Micic, Jim Murphy, Mark Hanna, Pingrong Yu, Alexander L. Efros, and Andrew Shabaev.

A. Martí and A. Luque acknowledge E. Antolín, E. Cánovas, N. López, C. Stanley, C. Farmer, and P. Díaz for their valuable discussions. Their work has been supported by the European Commission with the project FULLSPECTRUM (SES6-CT-2003–502620) and the projects NUMANCIA (S-0505/ENE/000310) funded by the Comunidad de Madrid and GENESISFV (CSD2006–0004) funded by the Spanish National Programme.

References

1. W. Shockley and H.J. Queisser, *J. Appl. Phys.* **32** (1961) p. 510.
2. A.J. Nozik, *Annu. Rev. Phys. Chem.* **52** (2001) p. 193.
3. R.T. Ross and A.J. Nozik, *J. Appl. Phys.* **53** (1982) p. 3813.
4. D.S. Boudreaux, F. Williams, and A.J. Nozik, *J. Appl. Phys.* **51** (1980) p. 2158.
5. P.T. Landsberg, H. Nussbaumer, and G. Willeke, *J. Appl. Phys.* **74** (1993) p. 1451.
6. S. Kolodinski, J.H. Werner, T. Wittchen, and H.J. Queisser, *Appl. Phys. Lett.* **63** (1993) p. 2405.
7. R.J. Ellingson, M.C. Beard, J.C. Johnson, P. Yu, O.I. Micic, A.J. Nozik, A. Shabaev, and A.L. Efros, *Nano Lett.* **5** (2005) p. 865.
8. M.C. Hanna and A.J. Nozik, *J. Appl. Phys.* **100** 074510 (2006).
9. A. Luque and A. Martí, *Phys. Rev. Lett.* **78** (1997) p. 5014.
10. A. Luque and A. Martí, *Prog. Photovoltaics: Res. Appl.* **9** (2001) p. 73.
11. J. Bude and K. Hess, *J. Appl. Phys.* **72** (1992) p. 3554.
12. H.K. Jung, K. Taniguchi, and C. Hamaguchi, *J. Appl. Phys.* **79** (1996) p. 2473.
13. D. Harrison, R.A. Abram, and S. Brand, *J. Appl. Phys.* **85** (1999) p. 8186.
14. O. Christensen, *J. Appl. Phys.* **47** (1976) p. 690.
15. M. Wolf, R. Brendel, J.H. Werner, and H.J. Queisser, *J. Appl. Phys.* **83** (1998) p. 4213.
16. R. Schaller and V. Klimov, *Phys. Rev. Lett.* **92** 186601 (2004).
17. J.E. Murphy, M.C. Beard, A.G. Norman, S.P. Ahrenkiel, J.C. Johnson, P. Yu, O.I. Micic, R.J. Ellingson, and A.J. Nozik, *J. Am. Chem. Soc.* **128** (2006) p. 3241.
18. A. Shabaev, Al.L. Efros, and A.J. Nozik, *Nano Lett.* **6** (2006) p. 2856.

19. R.D. Schaller, M. Sykora, J.M. Pietryga, and V.I. Klimov, *Nano Lett.* **6** (2006) p. 424.
20. R.D. Schaller, M.A. Petruska, and V.I. Klimov, *Appl. Phys. Lett.* **87** 253102 (2005).
21. R.D. Schaller, V.M. Agranovich, and V.I. Klimov, *Nature Phys.* **1** (2005) p. 189.
22. A. Franceschetti, J.M. An, and A. Zunger, *Nano Lett.* **6** (2006) p. 2191.
23. A. Hagfeldt and M. Grätzel, *Acc. Chem. Res.* **33** (2000) p. 269.
24. J. Moser, P. Bonnote, and M. Grätzel, *Coord. Chem. Rev.* **171** (1998) p. 245.
25. M. Grätzel, *Prog. Photovoltaics* **8** (2000) p. 171.
26. A. Zaban, O.I. Micic, B.A. Gregg, and A.J. Nozik, *Langmuir* **14** (1998) p. 3153.
27. R. Vogel and H. Weller, *J. Phys. Chem.* **98** (1994) p. 3183.
28. H. Weller, *Ber. Bunsen-Ges. Phys. Chem.* **95** (1991) p. 1361.
29. D. Liu and P.V. Kamat, *J. Phys. Chem.* **97** (1993) p. 10769.
30. P. Hoyer and R. Könenkamp, *Appl. Phys. Lett.* **66** (1995) p. 349.
31. N.C. Greenham, X. Peng, and A.P. Alivisatos, *Phys. Rev. B* **54** (1996) p. 17628.
32. N.C. Greenham, X. Peng, and A.P. Alivisatos, "A CdSe Nanocrystal/MEH-PPV Polymer Composite Photovoltaic" in *Future Generation Photovoltaic Technologies: First NREL Conf.*, edited by R. McConnell (AIP, 1997) p. 295.
33. W.U. Huynh, X. Peng, and P. Alivisatos, *Adv. Mater.* **11** (1999) p. 923.
34. A. Luque, A. Martí, and L. Cuadra, *IEEE Trans. Electron Dev.* **50** (2003) p. 447.
35. A. Luque, A. Martí, and L. Cuadra, *Physica E* **14** (2002) p. 107.
36. A. Luque, A. Martí, and L. Cuadra, *IEEE Trans. Electron Dev.* **48** (2001) p. 2118.
37. A. Luque, A. Martí, E. Antolín, and C. Tablero, *Physica B* **382** (2006) p. 320.
38. A. Martí, L. Cuadra, and A. Luque, in *Proc. 28th IEEE Photovoltaics Specialists Conf.* (IEEE, Piscataway, NJ, 2000) p. 940.
39. N.F. Mott, *Rev. Mod. Phys.* **40** (1968) p. 677.
40. A.J. Nozik, in *The Next Generation Photovoltaics: High Efficiency through Full Spectrum Utilization,* edited by A. Martí, A. Luque (Institute of Physics, Bristol, UK, 2003) p. 196.
41. U. Woggon, in *Optical Properties of Semiconductor Quantum Dots, Springer Tracts in Modern Physics* (Springer-Verlag, Heidelberg, 1996) p. 115.
42. K. Mukai and M. Sugawara, in *Self-Assembled InGaAs/GaAs Quantum Dots, Semiconductors and Semimetals, Vol. 60,* edited by M. Sugawara (Academic Press, San Diego, 1999) p. 209.
43. A. Martí, L. Cuadra, and A. Luque, *IEEE Trans. Electron Dev.* **48** (2001) p. 2394.
44. Y. Nakata, Y. Sugiyama, and M. Sugawara, in *Self-Assembled InGaAs/GaAs Quantum Dots, Semiconductors and Semimetals, Vol. 60,* edited by M. Sugawara (Academic Press, San Diego, 1999) p. 117.
45. A. Luque, A. Martí, N. López, E. Antolín, E. Cánovas, C. Stanley, C. Farmer, L.J. Caballero, L. Cuadra, and J.L. Balenzategui, *Appl. Phys. Lett.* **87** 083505 (2005).
46. A. Luque, A. Martí, N. López, E. Antolín, E. Cánovas, C.R. Stanley, C. Farmer, and P. Díaz, *J. Appl. Phys.* **99** 094503 (2006).
47. A. Luque, A. Martí, C. Stanley, N. López, L. Cuadra, D. Zhou, and A. McKee, *J. Appl. Phys.* **96** (2004) p. 903.
48. A.J. Nozik, *Physica E* **14** (2002) p. 115.
49. R.J. Ellingson, J.L. Blackburn, M. Beard, O.I. Micic, P. Yu, J. Murphy, and A.J. Nozik, in *Proc. ECS Meet.*, edited by T. Lian, K. Murakoshi, and G. Rumbles (San Antonio, 2004). □